ELSEVIER

Chemical Engineering Journal 75 (1999) 177–182

Chemical Engineering Journal

www.elsevier.com/locate/cej

A numerical study of the hydrodynamics of a falling liquid film on the internal surface of a downward tapered cone

Osamah Al-Hawaj

Department of Mechanical and Industrial Engineering, Kuwait University, P.O. Box 5969, Safat 13060, Kuwait

Received 16 September 1998; received in revised form 2 June 1999; accepted 15 June 1999

Abstract

The hydrodynamics of a falling laminar liquid film along the internal surface of a downward tapered cone in a stagnant vapor phase is presented. A marching procedure is employed for the solution of the equations of continuity, momentum and global mass for the two fluid velocity components u and v, and the film thickness, δ, in the entrance region and the asymptotically fully developed region. A parametric study illustrating the effects of the half-cone angle ϕ, inlet cone curvature, β, inlet Reynolds number, Re_0, and the inlet Froude number, Fr_0, on the streamwise distribution of film thickness, and wall skin friction are examined in detail. The obtained numerical results are compared with analytical results for special cases of the problem and are found to be in excellent agreement.

Keywords: Falling film; Hydrodynamics

1. Introduction

Liquid films flowing over vertical and inclined surfaces under the influence of gravity are encountered in many types of heat and mass transfer equipment: distillation columns, evaporators, wetted wall columns, diffusion processes of gases into a falling film and for cooling processes of hot walls.

Due to their technical importance, the literature contains numerous analytical and experimental results connected with laminar and turbulent flows of falling liquid films over flat plate, inclined plane, wavy inclined plane, inside pipes and outside pipes. For instance, Fulford [1] provides a summary of work done on the laminar fully developed flow over a semi-infinite plate. Limberg [2] investigated the turbulent analog. Nimmo [3] investigated the thin liquid film on curved surfaces. Rahman and Faghri [4] investigated the heat and mass transfer of a falling liquid film on the outer surface of a wedge and a cone in porous media. Ruckensein [5] investigated the diffusion and evaporation of a liquid film in rotary cone still. Anon [6] studied the performance of thin film evaporator in the shape of truncated cone, where liquid is introduced at the bottom of a cone and flow upward by the action of centrifugal forces.

However, the flow of a falling film flowing downward on the internal surface tapered cone has neither been studied theoretically nor experimentally. This type of geometry finds numerous applications in the chemical industrial processes including processes of evaporation and concentration of liquid solutions.

The problem at hand is concerned with the hydrodynamics of a laminar falling liquid film on the internal surface of a downward tapered cone. The film is assumed to issue from a slit opening at the upper edge of the cone with a parabolic velocity profile and flowing parallel to the cone surface. The film is considered to be sufficiently thin such that a boundary-layer approximation to the momentum equation is valid. Moreover, the Reynolds number is taken to be sufficiently small so that a laminar regime is maintained over the computational domain. The mathematical model consisting of the two-dimensional boundary layer, continuity equations and the equation for the local thickness based on overall mass balance is formulated and solved numerically. Prediction of the velocity profiles, thickness profiles, skin friction, local flow rate distribution is made. The influences of the effects of the half cone angle, ϕ, inlet cone curvature, β, inlet Reynolds number, Re_0, and inlet Froude number, Fr_0, on the solutions are investigated.

1385-8947/99/$ – see front matter
PII: S1385-8947(99)00089-3

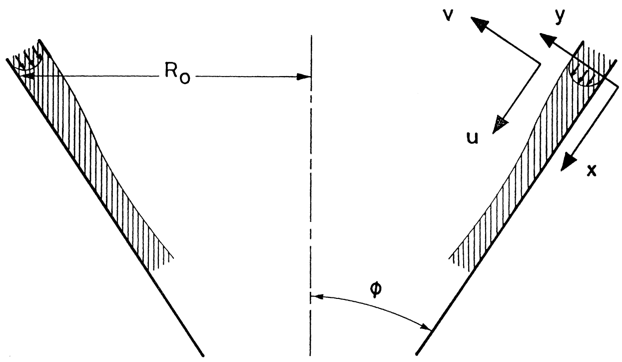

Fig. 1. Schematic of liquid falling film in a downward tapered cone.

2. Mathematical formulation

Fig. 1 illustrates the assumed flow region for steady laminar flow of an incompressible Newtonian fluid over the inner surface of a downward converging cone. The *X*-coordinate is taken along the surface of the cone and *Y*-coordinate is perpendicular to the cone surface with the origin taken at the slit opening.

The flow is assumed to be axisymmetric and the combination of minimum cone curvature parameter, Reynolds number and Froude number are such that the effect of capillary forces is negligible. The maximum liquid film thickness is at the truncated end, the *y*-velocity component are very small compared to local cone radius and *x*-velocity components, such that the boundary layer equations form are still valid. Furthermore, The effect of converging geometry is taken into account through a global mass conservation, one can express the two-dimensional boundary-layer and continuity equations as follows:

Continuity:

$$\frac{\partial}{\partial X}(RU) + \frac{\partial}{\partial Y}(RV) = 0 \tag{1}$$

X-momentum:

$$U\frac{\partial U}{\partial X} + V\frac{\partial U}{\partial Y} = g_x + \nu\frac{\partial^2 U}{\partial Y^2} \tag{2}$$

global mass balance:

$$Q = 2\pi\int_0^{\delta^*} RU\,\mathrm{d}Y \tag{3}$$

where Q is the volumetric obtained from the inlet condition as $Q = 2\pi R_0 U_0$, δ^* is the local film thickness and R is the local cone radius. The local cone radius R can be expressed from the cone geometry as a function of the local coordinate X, cone half angle ϕ and the initial cone radius R_0 as

$$R = R_0 - X\sin\phi \tag{4}$$

The liquid discharging from a two-dimensional slit is assumed to have a fully parabolic velocity profile and the liquid interface is under negligible shear stress such that the inlet and boundary conditions are expressed as follows:

$$U(0,Y) = 6U_0\left(\frac{Y}{\delta_0}\right)\left(1-\frac{Y}{\delta_0}\right), \qquad V(0,Y) = 0 \tag{5}$$

$$U(X,0) = V(X,0) = 0 \tag{6}$$

$$\frac{\partial U(X,\delta^*)}{\partial Y} = 0 \tag{7}$$

where U_0 and δ_0 are the initial average velocity and initial film thickness. It is convenient to employ the following normalized variables:

$$x = \frac{X}{\delta_0}, \qquad y = \frac{Y}{\delta^*(x)}, \qquad u = \frac{U}{U_0}, \qquad v = \frac{V}{U_0},$$
$$\delta(x) = \frac{\delta^*(x)}{\delta_0} \tag{8}$$

Substituting Eq. (8) into Eqs. (1)–(7) results in the following dimensionless equations:

$$\frac{\partial}{\partial x}[(\beta - x\sin\phi)u] + \frac{\partial}{\partial y}[(\beta - x\sin\phi)v] = 0 \tag{9}$$

$$\frac{\partial^2 u}{\partial y^2} - Re_0\,\delta^2 u\frac{\partial u}{\partial x} - Re_0\,\delta v\frac{\partial u}{\partial y} + \frac{Re_0}{Fr_0^2}\delta^2\cos\phi = 0 \tag{10}$$

$$\delta = \frac{1}{(1-((x/\beta)\sin\phi))\int_0^1 u\,\mathrm{d}y} \tag{11}$$

where $Re_0 = U_0\delta_0/\nu$, $\beta = R_0/\delta_0$ and $Fr_0^2 = U_0^2/g\delta_0$ are the inlet Reynolds number, inlet cone curvature parameter and the square of the inlet Froude number, respectively.

The dimensionless boundary conditions become

$$u(0,y) = 6y(1-y), \qquad v(0,y) = 0, \qquad \delta(0) = 1 \tag{12}$$

$$u(x,0) = v(x,0) = 0 \tag{13}$$

$$\frac{\partial u(x,1)}{\partial x} = 0. \tag{14}$$

3. Numerical solution

The governing equations and boundary conditions were converted into a finite difference form and solved numerically on a digital computer using a 'marching ahead' scheme. The numerical computation starts at the leading upper edge, i.e. $x = 0$, and terminates when the local Reynolds number reached the critical Reynolds number for a falling film on a flat plate. It is assumed that the critical Reynolds number is negligibly affected by the effect of cone curvature. At any given x position, the x-momentum Eq. (10) is solved for the u velocity component by a tri-diagonal method followed by solving for the v velocity component directly from the continuity Eq. (9). At each x position, the global mass conservation is enforced and the normalized film thickness δ is calculated from Eq. (11). Convergence of the solution is considered achieved when all changes in the velocity components and the film thickness between two successive iterations is less than 1×10^{-4}. The computational grid used for this study is rectangular with the normalized coordinate is scaled by the variable film thickness, δ^*. A fine grid is used in the entrance region and near the wall to account for the rapid variation in the film thickness and the x-velocity component.

4. Results and discussion

4.1. Model validation

In the absence of experimental and analytical results for the general problem of a falling liquid film in a cone geometry, the numerical results are compared with the analytical solution obtained for large x and when the inlet cone curvature parameter, β, becomes large. In this case, the flow corresponds to the case of the fully developed region in which all gradient terms with respect to x and the vertical y velocity component, v, vanishes and thereby Eqs. (9)–(14) reduce to:

$$\frac{\mathrm{d}^2u}{\mathrm{d}y^2} + \delta^2 \frac{Re_0 \cos\phi}{Fr_0^2} = 0 \tag{15}$$

$$u(0) = 0 \tag{16}$$

$$\frac{\mathrm{d}u}{\mathrm{d}y}(1) = 0 \tag{17}$$

The above equations are solved by direct integration to give the following solution:

$$u(y) = C_0 y\left(1-\frac{y}{2}\right) \tag{18}$$

where

$$C_0 = \frac{3^{2/3} Re_0^{1/3} \cos\phi^{1/3}}{Fr_0^{2/3}}$$

A special film asymptotic thickness, δ, for the special case is obtained for large inlet cone curvature, β, whereby Eq. (11) reduces to

$$\delta \int_0^1 u\,\mathrm{d}y = 1 \tag{19}$$

Substituting Eq. (18) into Eq. (19) obtains the asymptotic film thickness as

$$\delta = \frac{3^{1/3} Fr_0^{2/3}}{Re_0^{1/3} \cos\phi^{1/3}} \tag{20}$$

Fig. 2 compares the analytical solution as given by Eq. (18) and the numerical solution for the inlet cone curvature parameter, $\beta = 10\,000$ at streamwise distance $x = 300$, which indicates excellent agreement.The wall skin friction coefficient, f, is obtained from the definition as

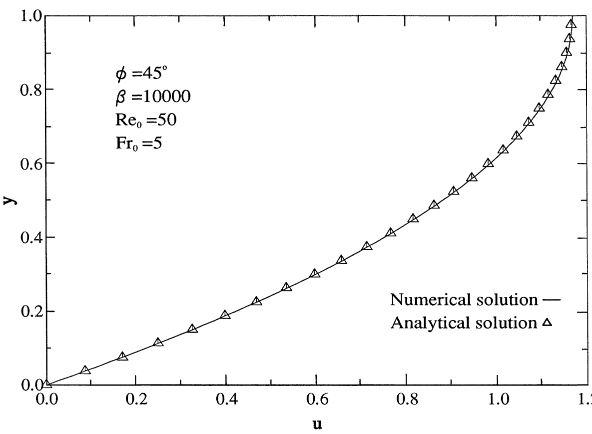

Fig. 2. Axial velocity profiles comparison for large initial cone curvature.

$$f = \frac{\tau_w}{(1/2)\rho U_0^2} = \frac{2}{Re_0\,\delta}\left[\frac{\partial u}{\partial y}\right]_{y=0} \tag{21}$$

By substituting Eqs. (18) and (20) into Eq. (21), the asymptotic friction factor for large inlet cone curvature, β, becomes

$$f = \frac{2.88 \cos\phi^{2/3}}{Re_0^{1/3} Fr_0^{4/3}} \tag{22}$$

4.2. Velocity profiles

Fig. 3 presents the u-velocity profiles development in the entrance region for prescribed values of reference values of the inlet Reynolds number, $Re_0 = 50$, half cone angle, $\phi = 45^\circ$, inlet cone curvature, $\beta = 500$, and inlet Froude number, $Fr_0 = 5$. Those reference parameters are chosen to conform to the assumptions of laminar regime and negligible capillary effects, in addition to being representative values in practical applications. The velocity profile starts with a fully parabolic velocity profile as it exits a two-

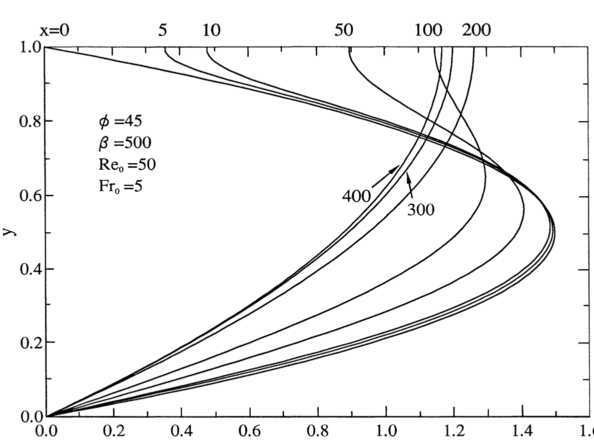

Fig. 3. Axial development of u-velocity profiles.

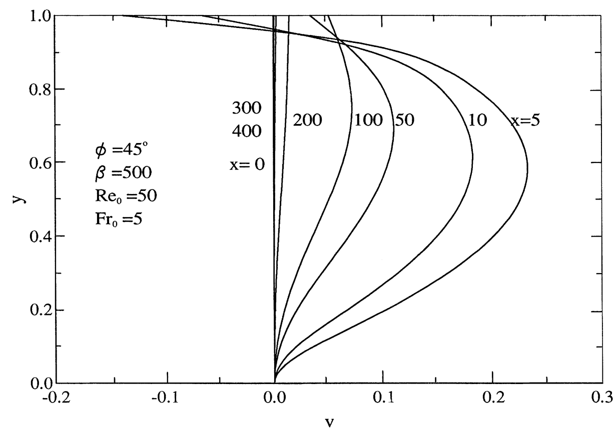

Fig. 4. Axial development of v-velocity profiles.

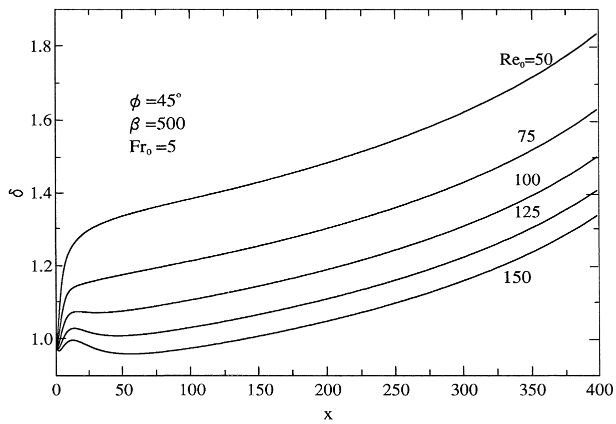

Fig. 6. Effect of inlet Reynolds number on axial film thickness distribution.

dimensional slit surrounding the upper rim of the cone and undergoes an adjustment to a half parabolic velocity profile. The numerical solution indicates the existence of self-similar velocity profiles of the form $u/U_0 = f(y/\delta)$ in the asymptotic region.

Fig. 4 presents the corresponding v-velocity profiles development in the entrance region under the same conditions. Initially the velocity profile starts having zero v-component as it exits the slit, and then undergoes a region of an adjustment to become asymptotically self-similar. The non-vanishing of the v-velocity profiles for large streamwise distance is due to the growth of the liquid film thickness. The values of the velocity close to the interface indicate a sharp dip followed by a sudden increase in the film thickness diminishing to asymptotically small value.

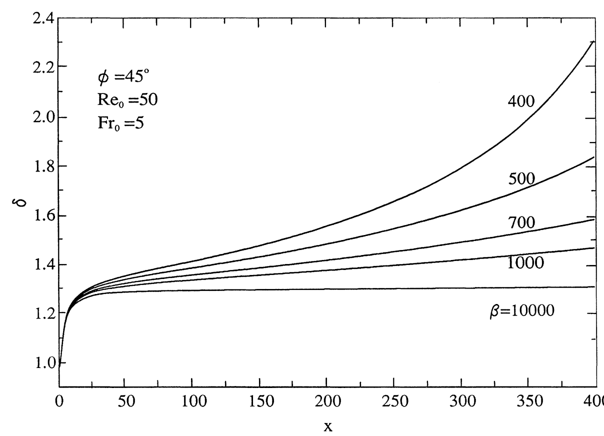

Fig. 7. Effect of initial cone curvature on axial film thickness distribution.

4.3. Film thickness distributions

Figs. 5–8 demonstrate the general trend and the effect of the cone half angle, ϕ, inlet Reynolds number, Re_0, inlet cone curvature, β, and the inlet Froude number, Fr_0, on the film thickness distribution. These effects are in agreement

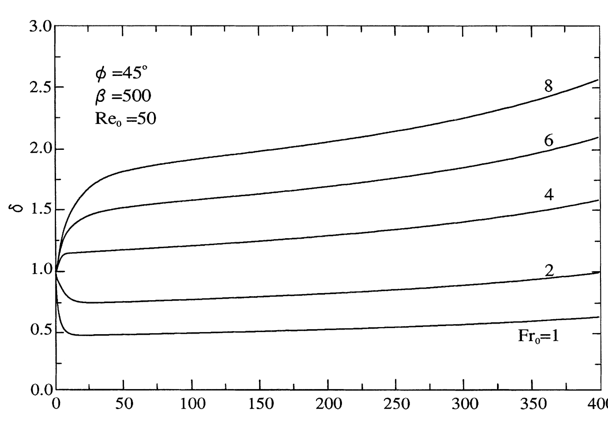

Fig. 8. Effect of inlet Froude number on axial film thickness distribution.

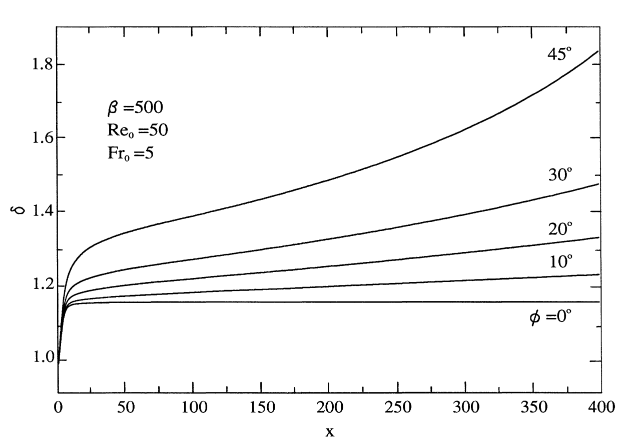

Fig. 5. Effect of cone half angle on axial film thickness distribution.

with expected trends obtained for the special case given in Eq. (20). Generally speaking, except for the short entrance region, the film thickness shows monotonic increase in the direction of the flow due to cone tapering and the associated decrease in wetted area. The film thickness decreases with increase in the inlet Reynolds number, Re_0, and inlet cone curvature, β; while it increases with increase in the half cone angle, ϕ, and the inlet Froude number, Fr_0. Two special cases are included in the results for which the asymptotic film thickness remains constant. The first case is when the half angle is equal to zero which corresponds to a vertical cylindrical conduit and the second case when curvature is very large which closely approximates to an inclined flat plate.

4.4. Skin friction

Figs. 9–12 demonstrate the general trend and the effect of the cone half angle, ϕ, inlet Reynolds number, Re_0, inlet cone curvature, β, and the inlet Froude number, Fr_0, on the skin friction distribution $f(x)$. These effects are in agreement with expected trends obtained for the special case given in Eq. (22). Excluding the short entrance region, and for a given set of parameters, the wall skin friction coefficient increases in the flow direction with increasing distance from the inlet. The effect of increasing half cone angle, ϕ, inlet Reynolds number, Re_0, inlet cone curvature, β, and the inlet Froude number, Fr_0, is found to decrease the skin friction coefficient.

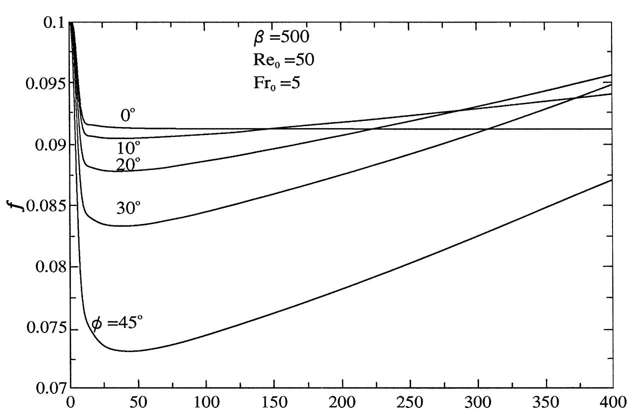

Fig. 9. Effect of cone half angle on axial wall skin friction distribution.

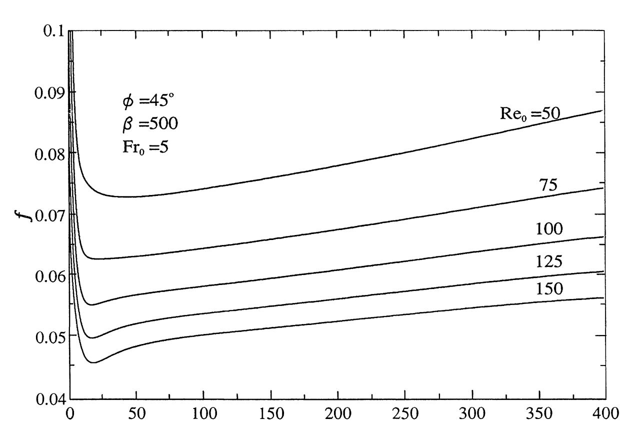

Fig. 10. Effect of inlet Reynolds number on wall skin friction distribution.

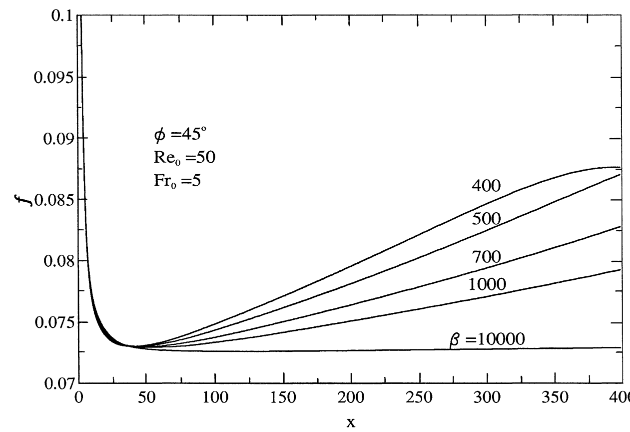

Fig. 11. Effect of initial cone curvature on wall skin friction distribution.

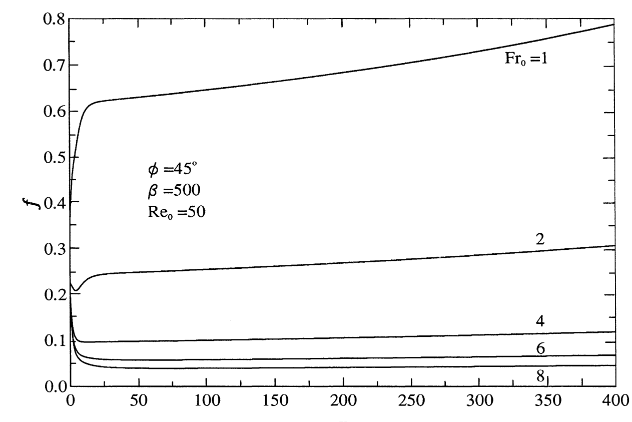

Fig. 12. Effect of inlet Froude number on the wall skin friction distribution.

5. Conclusion

The hydrodynamics of steady, laminar falling liquid film on the internal surface of downward tapered cone is studied numerically using a marching technique. The obtained results for special cases are in excellent agreement with analytical solutions. It was found that the film thickness and skin friction depended on the inlet flow parameters, cone half angle and the distance from the inlet. The film thickness and skin friction increase with the distance from the inlet for tapered cones. The effect of increasing the inlet Reynolds number was found to decrease the film thickness and the skin friction. The effect of increasing the inlet Froude number was predicted to increase the film thickness and to decrease the skin friction coefficient. The effect of increasing the half cone angle was shown to increase the film thickness and to decrease the skin friction coefficient. Both the film thickness and the skin friction were predicted to decrease as a result of increasing the inlet cone curvature. Moreover, the numerical solution reduced to two special cases, namely, for zero half cone angle corresponding to vertical cylindrical conduit, and for large inlet cone curvature corresponding to an inclined flat plate.

References

[1] G.D. Fulford, The flow of liquids in thin films, in: Advances in Chemical Engineering, vol. 5, Academic Press, New York, 1964, p. 151.

[2] H. Limberg, Turbulent flow of a falling liquid film, Archiwum Mechaniki Stosowanej 241 (1972) 35–42.

[3] B. Nimmo, Thin film flow on curved surfaces, Journal of Engineering Science 27 (1972) 695–701.

[4] M.M. Rahman, A. Faghri, Transport in a thin liquid film on the outer surface of a wedge or cone embedded in a porous medium Part 1: mathematical analysis, International Communications in Heat and Mass Transfer 201 (1993) 15–27.

[5] E. Ruckenstein, W.J. Hassink, The combined effect of diffusion and evaporation on the molecular distillation of ideal binary liquid mixtures, Separation Science and Technology 186 (1983) 523–545.

[6] Anon, High performance thin film evaporator, in: Proc. Technology, vol. 18, 1973, p. 19.